Journal of Sound and Vibration (1999) **224**(4), 625–642
Article No. jsvi.1999.2206, available online at http://www.idealibrary.com on IDEAL®

FREE BENDING VIBRATION OF A MULTI-STEP ROTOR

O. S. JUN

Department of Mechanical Engineering, Jeonju University, Jeonju 560-759, *Korea*

AND

J. O. KIM

Department of Mechanical Engineering, Soongsil University, Dongjak-gu, Seoul 156-743, *Korea*

(*Received* 22 *January* 1998 *and in final form* 19 *January* 1999)

The free bending vibration of a rotating shaft composed of multi-step segments with each segment having a uniform circular cross-section has been analyzed using the Timoshenko beam model. Torque has been applied at each end as in a power-transmission shaft and the gyroscopic effect due to the shaft rotation has also been considered. The separation of time and spatial variables has been performed for the differential equation of motion, and then the spatial solution in a segment of uniform cross-section has been expressed in a closed form. Application of boundary conditions has induced global equations of a rotor system, from which the natural frequencies and corresponding mode shapes have been obtained. The entire procedure is straightforward, and thus the resultant mode shapes are continuous unlike the result of existing methods such as the finite element method and transfer matrix method. Effects of the rotating speed and the applied torque at both ends on the free vibration of the rotating shaft have been discussed. The natural frequencies of the forward and backward modes have been compared with the results using the finite element method. The shear force and bending moment distributions along the shaft at each mode have been derived by differentiating the mode curves.

1. INTRODUCTION

Vibrations of rotating bodies result from various sources. Most of the vibration sources are extrinsic anomalies such as unbalance and misalignment, and some of the sources are intrinsic factors such as bearing or shaft asymmetries. Since the vibration sources exist unavoidably in rotating bodies as vibrating systems, it is important to obtain the natural vibration characteristics for designing rotating shafts. If a synchronous or non-synchronous component in the vibration spectrum of the shaft coincides with a natural frequency, the shaft does not work normally due to resonance.

The vibration of general rotating shaft is analyzed usually by the finite element method or transfer matrix method. These methods calculate physical parameter values, for example displacements, at nodal points, and they provide accurate but discontinuous mode-shape curves. Other approaches [1, 2] to obtain continuous

0022-460X/99/290625 + 18 $30.00/0

mode-shape curves have been reported for bending or torsional vibrations, but the approach for bending vibration has limitations because the analysis is based on the Euler–Bernoulli beam theory [1], which does not include the rotary inertia and shear deformation of the cross-sections. The effect of the rotary inertia and shear deformation reduces the fundamental natural frequency by 0·3% in a uniform beam with a radius-to-length ratio of 1 : 20, and the effect is bigger for higher modes [3]. The larger the radius-to-length ratio, the bigger the effect of the rotary inertia and shear deformation is on the fundamental natural frequency. Thus, the Timoshenko beam theory, which includes the rotary inertia and shear deformation of the cross-section, is applied to a general rotating shaft for an accurate analysis.

In this paper, a general rotating shaft is considered as a multi-step shaft model with each step having a uniform cross-section. Torque is applied at each end as in a power-transmission shaft and the gyroscopic effect due to the shaft rotation is also included in the equation of motion based on the Timoshenko beam theory. During the analysis of the free bending vibration, two vertical displacements are expressed as one complex variable and separation of time and spatial variables is introduced. By solving the resulting polynomial equation and applying boundary conditions, natural frequencies and continuous mode-shape curves are obtained for the general rotating shaft. The continuous mode shape curve is used to calculate shear force and bending moment distributions.

2. PROBLEM FORMULATION

The elastodynamic behavior of a thick uniform shaft is described by considering the rotary inertia and shear deformation of the cross-section, like the general beam theory. Especially for the rotating shaft, the gyroscopic effect due to the rotation is also considered. With the torque in a power-transmitting shaft included, the equation of motion of the rotating shaft is written as follows [4]:

$$EI\frac{\partial^4 y}{\partial x^4} - \frac{EI\rho}{\kappa G}\frac{\partial^4 y}{\partial x^2 \partial t^2} + T\frac{\partial^3 z}{\partial x^3} - \frac{T\rho}{\kappa G}\frac{\partial^3 z}{\partial x \partial t^2} + \rho A\frac{\partial^2 y}{\partial t^2}$$

$$- \rho A r_o^2\left[\left(\frac{\partial^4 y}{\partial x^2 \partial t^2} - \frac{\rho}{\kappa G}\frac{\partial^4 y}{\partial t^4}\right) + 2\Omega\left(\frac{\partial^3 z}{\partial x^2 \partial t} - \frac{\rho}{\kappa G}\frac{\partial^3 z}{\partial t^3}\right)\right] = 0, \tag{1a}$$

$$EI\frac{\partial^4 z}{\partial x^4} - \frac{EI\rho}{\kappa G}\frac{\partial^4 z}{\partial x^2 \partial t^2} - T\frac{\partial^3 y}{\partial x^3} + \frac{T\rho}{\kappa G}\frac{\partial^3 y}{\partial x \partial t^2} + \rho A\frac{\partial^2 z}{\partial t^2}$$

$$- \rho A r_o^2\left[\left(\frac{\partial^4 z}{\partial x^2 \partial t^2} - \frac{\rho}{\kappa G}\frac{\partial^4 z}{\partial t^4}\right) - 2\Omega\left(\frac{\partial^3 y}{\partial x^2 \partial t} - \frac{\rho}{\kappa G}\frac{\partial^3 y}{\partial t^3}\right)\right] = 0, \tag{1b}$$

where x is the axial co-ordinate and y and z are the displacements in the horizontal and vertical directions respectively. T is the torque on each end of the shaft, and E, G, and ρ are Young's modulus, shear modulus, and mass density respectively. A and

I are the area and area moment of inertia of the cross-section, r_0 is the radius of gyration, κ is the form factor, and Ω is the rotating speed.

Since equations (1) are coupled, the solution of y and z cannot be obtained simply. To avoid solving the coupled equations the dynamic behavior in the x–y and x–z planes can be expressed by one equation in terms of the following complex variable:

$$u(x, t) = y(x, t) + \mathrm{j}z(x, t). \tag{2}$$

By using $u(x, t)$ of equation (2), equation (1) is reduced to one equation as follows:

$$EI\frac{\partial^4 u}{\partial x^4} - \frac{EI\rho}{\kappa G}\frac{\partial^4 u}{\partial x^2 \partial t^2} - \mathrm{j}T\frac{\partial^3 u}{\partial x^3} + \mathrm{j}\frac{T\rho}{\kappa G}\frac{\partial^3 u}{\partial x \partial t^2} + \rho A\frac{\partial^2 u}{\partial t^2}$$

$$- \rho A r_o^2\left[\left(\frac{\partial^4 u}{\partial x^2 \partial t^2} - \frac{\rho}{\kappa G}\frac{\partial^4 u}{\partial t^4}\right) - \mathrm{j}2\Omega\left(\frac{\partial^3 u}{\partial x^2 \partial t} - \frac{\rho}{\kappa G}\frac{\partial^3 u}{\partial t^3}\right)\right] = 0. \tag{3}$$

Equation (3) can be reordered according to the order of the derivatives with respect to x as follows:

$$EI\frac{\partial^4 u}{\partial x^4} - \mathrm{j}T\frac{\partial^3 u}{\partial x^3} - \left(\frac{EI\rho}{\kappa G} + \rho A r_o^2\right)\frac{\partial^4 u}{\partial x^2 \partial t^2} + \mathrm{j}2\rho A r_o^2 \Omega\frac{\partial^3 u}{\partial x^2 \partial t} + \mathrm{j}\frac{T\rho}{\kappa G}\frac{\partial^3 u}{\partial x \partial t^2}$$

$$+ \frac{\rho^2 A r_o^2}{\kappa G}\frac{\partial^4 u}{\partial t^4} - \mathrm{j}2\frac{\rho^2 A r_o^2 \Omega}{\kappa G}\frac{\partial^3 u}{\partial t^3} + \rho A\frac{\partial^2 u}{\partial t^2} = 0. \tag{4}$$

which is a fourth order partial differential equation of $u(x, t)$.

Meanwhile, the boundary conditions are expressed in terms of the displacement, slope of the shaft, bending moment, and shearing force as follows [2]:

$$\text{displacement} \quad u(x, t), \tag{5a}$$

$$\text{slope} \quad \frac{\partial u}{\partial x}, \tag{5b}$$

$$\text{bending moment} \quad EI\frac{\partial^2 u}{\partial x^2} - \mathrm{j}T\frac{\partial u}{\partial x}, \tag{5c}$$

$$\text{shearing force} \quad EI\frac{\partial^3 u}{\partial x^3} - \mathrm{j}T\frac{\partial^2 u}{\partial x^2} - \rho A r_o^2\left(\frac{\partial^3 u}{\partial x\, \partial t^2} - 2\mathrm{j}\Omega\frac{\partial^2 u}{\partial x \partial t}\right). \tag{5d}$$

3. ANALYTICAL APPROACH

Equation (4) is solved analytically by separation of variables as follows.

3.1. SEPARATION OF VARIABLES

The time-dependent harmonic motion of natural frequency ω can be separated in the variable $u(x, t)$ as

$$u(x, t) = U(x)\mathrm{e}^{\mathrm{j}\omega t}. \tag{6}$$

Substituting equation (6) into equation (4) results in the following equation:

$$EI\frac{\mathrm{d}^4U}{dx^4} - \mathrm{j}T\frac{\mathrm{d}^3U}{\mathrm{d}x^3} + \left[\left(\frac{EI\rho}{\kappa G} + \rho A r_0^2\right)\omega^2 - 2\rho A r_o^2 \Omega\omega\right]\frac{\mathrm{d}^2U}{\mathrm{d}x^2}$$

$$-\mathrm{j}\frac{T\rho}{\kappa G}\omega^2\frac{\mathrm{d}U}{\mathrm{d}x} + \left[\frac{\rho^2 A r_o^2}{\kappa G}\omega^4 - 2\frac{\rho^2 A r_0^2 \Omega}{\kappa G}\omega^3 - \rho A\omega^2\right]U = 0. \tag{7}$$

Equation (7) is a fourth order ordinary differential equation of a complex variable U and complex coefficients in the following form:

$$\frac{\mathrm{d}^4U}{\mathrm{d}x^4} + a\frac{\mathrm{d}^3U}{\mathrm{d}x^3} + b\frac{\mathrm{d}^2U}{\mathrm{d}x^2} + c\frac{\mathrm{d}U}{\mathrm{d}x} + \mathrm{d}U = 0, \tag{8}$$

where

$$a = -\frac{\mathrm{j}T}{EI},$$

$$b = \frac{1}{EI}\left[\left(\frac{EI\rho}{\kappa G} + \rho A r_o^2\right)\omega^2 - 2\rho A r_0^2 \Omega\omega\right],$$

$$c = -\mathrm{j}\frac{1}{EI}\frac{T\rho}{\kappa G}\omega^2,$$

$$d = \frac{1}{EI}\left[\frac{\rho^2 A r_o^2}{\kappa G}\omega^4 - 2\frac{\rho^2 A r_o^2 \Omega}{\kappa G}\omega^3 - \rho A\omega^2\right]. \tag{9}$$

Equation (8) has solutions of the form of $U = p\mathrm{e}^{\lambda x}$, and substituting it into equation (8) yields the fourth order polynomials of λ, which is also complex:

$$\lambda^4 + a\lambda^3 + b\lambda^2 + c\lambda + d = 0. \tag{10}$$

3.2. SOLUTIONS OF THE FOURTH ORDER POLYNOMIAL

The fourth order polynomial of equation (10) has the following third order analytic equation [5]:

$$\mu^3 - b\mu^2 + (ac - 4d)\mu - a^2 d + 4bd - c^2 = 0. \tag{11}$$

Let a root of the third order polynomial equation for μ be μ_1 and

$$R = \left(\frac{a^2}{4} - b + \mu_1\right)^{1/2}. \tag{12}$$

Define D and E as

$$D = \left(\frac{3a^2}{4} - R^2 - 2b + \frac{4ab - 8c - a^3}{4R}\right)^{1/2}$$

$$E = \left(\frac{3a^2}{4} - R^2 - 2b - \frac{4ab - 8c - a^3}{4R}\right)^{1/2} \qquad \text{when } R \neq 0 \tag{13a}$$

and

$$D = \left(\frac{3a^2}{4} - 2b + 2(y^2 - 4d)^{1/2}\right)^{1/2}$$

$$E = \left(\frac{3a^2}{4} - 2b - 2(y^2 - 4d)^{1/2}\right)^{1/2} \qquad \text{when } R = 0. \tag{13b}$$

Then the roots of equation (10) can be written as

$$\lambda_1 = -\frac{a}{4} + \frac{R}{2} + \frac{D}{2},$$

$$\lambda_2 = -\frac{a}{4} + \frac{R}{2} - \frac{D}{2},$$

$$\lambda_3 = -\frac{a}{4} - \frac{R}{2} + \frac{E}{2},$$

$$\lambda_4 = -\frac{a}{4} - \frac{R}{2} - \frac{E}{2}. \tag{14}$$

The solution of equation (8) is expressed in terms of the root λ's as

$$U = p_1 e^{\lambda_1 x} + p_2 e^{\lambda_2 x} + p_3 e^{\lambda_3 x} + p_4 e^{\lambda_4 x}. \tag{15}$$

Equation (15) means that the elastodynamic behavior of the rotating shaft is dependent on λ's, which are determined by several parameters, such as rotating speed Ω, natural frequency ω, and geometric and material properties of the shaft.

The coefficients p_1, p_2, p_3, p_4 of equation (15) are also complex values defined in a uniform shaft segment.

3.3. MULTI-STEP SHAFT

The derivation shown above can be extended to the non-uniform shaft, like a multi-step shaft whose cross-section is uniform in each step. The deformation of the ith step segment can be expressed as

$$U_i = p_{i1}e^{\lambda_{i1}x} + p_{i2}e^{\lambda_{i2}x} + p_{i3}e^{\lambda_{i3}x} + p_{i4}e^{\lambda_{i4}x}. \tag{16}$$

At an interface of two steps, i.e., at the right end of the left element and the left of the right element, the continuity is maintained for the displacement, slope of the shaft, bending moment, and shearing force. This statement is written by using the expressions of equation (5) as

$$U|_L = U|_R, \tag{17a}$$

$$\left.\frac{dU}{dx}\right|_L = \left.\frac{dU}{dx}\right|_R, \tag{17b}$$

$$EI\frac{d^2U}{dx^2} - jT\left.\frac{dU}{dx}\right|_L = EI\frac{d^2U}{dx^2} - jT\left.\frac{dU}{dx}\right|_R, \tag{17c}$$

$$EI\frac{d^3U}{dx^3} - jT\frac{d^2U}{dx^2} + \rho Ar_o^2(\omega^2 - 2\omega\Omega)\left.\frac{dU}{dx}\right|_L$$

$$= EI\frac{d^3U}{dx^3} - jT\frac{d^2U}{dx^2} + \rho Ar_o^2(\omega^2 - 2\omega\Omega)\left.\frac{dU}{dx}\right|_R. \tag{17d}$$

Our attention is concentrated on the power-transmitting shaft, and the additional boundary conditions are classified and written in the Appendix A.

4. ANALYSIS RESULTS

Selecting adequate boundary conditions among equations (A1)–(A6) and applying them to the given system of a rotating shaft give equations for the full system. The equations consist of a matrix whose dimension is four times the number of shaft steps and of a vector $\{p_{11}, p_{12}, p_{13}, p_{14}, \cdots, p_{N1}, p_{N2}, p_{N3}, p_{N4}\}^T$. The matrix includes (2×4) submatrices obtained at each end and (4×8) submatrices obtained at the interfaces of the shaft steps. This homogeneous matrix equation is a characteristic value problem.

The homogeneous matrix equation has non-trivial solutions when the determinant of the matrix is zero. The roots ω's of the characteristic determinant equation are the natural frequencies of the shaft. The corresponding solutions p_{11}, p_{12}, p_{13}, p_{14}, $\ldots$, p_{N1}, p_{N2}, p_{N3}, p_{N4} are the coefficients determining the deformation of the shaft. In the analysis the values λ_{i1}, λ_{i2}, λ_{i3}, λ_{i4} defined in each step are also to be obtained in order to calculate the shaft deformation.

4.1. STATIONARY UNIFORM SHAFT WITH NO TORQUE

In order to confirm the accuracy of the analysis method, the natural frequencies of a uniform shaft have been calculated and compared with the corresponding values obtained from the Euler–Bernoulli beam theory. It has been assumed that the rotating speed Ω is zero and no torque T is exerted. The dimensions of the shaft considered for the calculation are length (l) 1 m and diameter (d) 50 mm. The material properties are Young's modulus (E) $2{\cdot}058 \times 10^{11}$ N/m^2, the Poisson ratio (v) 0·29, and mass density (ρ) 7800 kg/m^3.

The natural frequencies calculated for the shaft model equally divided into two and four elements respectively coincide with each other within four significant digits for the first three modes, and the results are shown in Table 1. The corresponding natural frequencies obtained by the following formula of the Euler–Bernoulli theory is also presented in Table 1:

$$\omega_n = \sqrt{\frac{EI}{\rho A}}\,\frac{n^2\pi^2}{l^2}. \tag{18}$$

The uniform shaft model used for the calculation has the aspect ratio (d/l) equal to 0·05. The difference between the two results is within 0·30% for the fundamental frequency. The difference is increased for higher modes, because the rotary inertia and shear deformation, which are neglected in the Euler–Bernoulli theory,

TABLE 1

Comparison of natural frequencies of the stationary uniform shaft with no torque, obtained from the Euler–Bernoulli beam theory and calculated by the analysis method presented in this paper

Mode	Natural frequency (Hz)	
	Euler–Bernoulli theory	This paper's method (using Timoshenko theory)
1st	100·9	100·6
2nd	403·4	399·6
3rd	907·7	888·1

contribute and reduce the natural frequency. This comparison supports the accuracy of the method of this paper.

4.2. STATIONARY MULTI-STEP SHAFT WITH NO TORQUE

As a first step of the analysis for the multi-step shaft model shown in Figure 1, the analysis method had been used to obtain the natural vibration characteristics of the stationary shaft. Thus it has been assumed that the rotating speed Ω is zero and no torque T is exerted. The dimensions of the shaft model shown in Figure 1 have been specified in Table 2. The material properties of the shaft are the same as mentioned in section 4.1.

In the multi-step shaft model, the interface between Element 1 and Element 2 is simply supported, and so is the end of Element 6. By applying these conditions and the cross-section jump conditions described in detail in the Appendix A, the equations for the entire system have been constructed in terms of the parameters p_{i1}, p_{i2}, p_{i3}, p_{i4} and λ_{i1}, λ_{i2}, λ_{i3}, λ_{i4} of the ith ($i = 1, 2, \ldots, 6$) uniform element.

The natural frequencies of the first four modes calculated by the analysis method described in section 3 are 268·7, 1104·1, 2411·8, and 4200·3 Hz. These are listed in r.p.m. unit in the first row of Table 3. In the table 'exact' indicates the results obtained by this study, while 'FEM' indicates the results obtained using the finite element method. This comparison shows a bigger error for a higher mode in the FEM result. The errors follow an increasing trend from the first mode = 0·089%, 0·38%, 2·82%, and 8·84%.

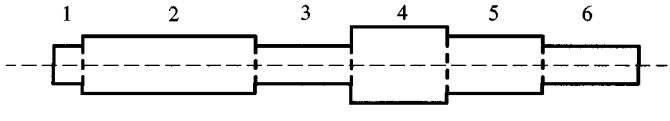

Figure 1. Multi-step shaft model and element numbers used for the analysis. The length and diameter of each element are listed in Table 2.

TABLE 2
Specification of the multi-step shaft model shown in Figure 1

Elements	Length (cm)	Diameter (cm)
1	3	4
2	17	5
3	10	4
4	10	6
5	10	5
6	10	4

TABLE 3

Natural frequency variation at each mode according to the rotating speed Ω for the multi-step shaft with no torque

Rotating speed Ω (r.p.m.)	Method	Natural frequencies (r.p.m.)							
		1st mode		2nd mode		3rd mode		4th mode	
		Backward	Forward	Backward	Forward	Backward	Forward	Backward	Forward
0	exact	16120·7		66246·1		144707·4		252016·8	
	FEM	16106·4		66497·2		148790·2		274316·6	
5000	exact	16099·9	16141·4	66144·5	66347·8	144549·6	144865·2	251706·0	252327·8
	FEM	16085·6	16127·1	66394·3	66600·2	148626·6	148954·0	273945·1	274688·7
10000	exact	16079·1	16162·3	66043·1	66449·6	144392·0	145023·1	251395·4	252639·1
	FEM	16064·9	16147·9	66291·7	66703·3	148463·1	149117·9	273574·1	275061·3
15000	exact	16058·4	16183·1	65941·8	66551·5	144234·5	145181·2	251085·1	252950·5
	FEM	16044·2	16168·7	66189·1	66806·6	148299·8	149282·1	273203·7	275434·4
20000	exact	16037·7	16203·9	65840·6	66653·6	144077·1	145339·3	250775·0	253262·4
	FEM	16023·5	16189·5	66086·7	66910·1	148136·7	149446·3	272833·8	275808·1

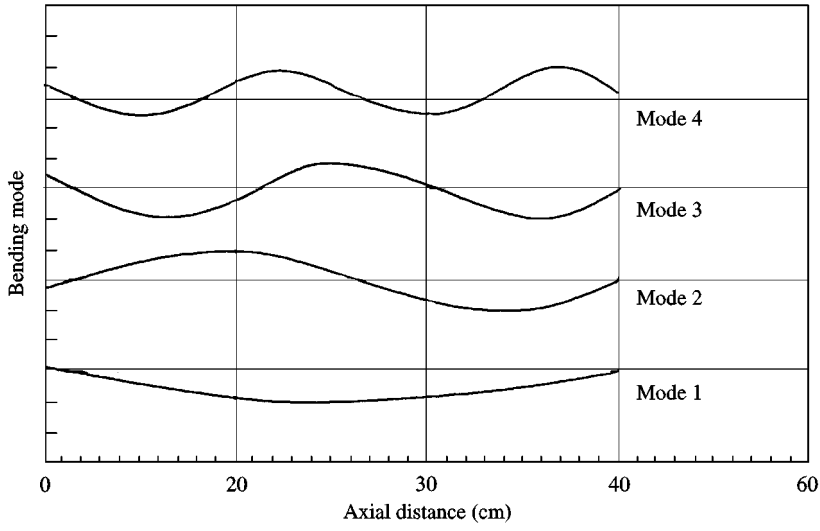

Figure 2. Normalized mode shapes of the first four natural modes of bending vibration.

4.3. ROTATING MULTI-STEP SHAFT WITH TORQUE

The natural frequencies of the rotating multi-step shaft with torque depend on the rotating speed and torque. The effect of rotation on the natural frequency has been examined by fixing the torque at zero and considering various rotation speeds from 0 to 20,000 r.p.m. The natural frequencies calculated for the forward and backward precessions of the first four modes are listed in r.p.m. units in Table 3, which shows an increase of the natural frequency for the forward precession and a decrease for the backward precession. This phenomenon is understood as the stiffening and softening of the gyroscopic effect. These results are compared with the results obtained by using the finite element method. The separation of the natural frequencies of the forward and backward precessions with increasing rotating speed is consistent with the finite element method result in the sense of the trend and the magnitude. The mode shapes corresponding to the natural modes listed in Table 3 are shown in Figure 2. Timoshenko beam theory has been applied to the shaft of stepped cross-sections, and the mode shapes have been obtained as continuous curves. It appears that there is no variation of the mode shape according to the rotating speed.

The effect of torque has been examined by fixing the rotating speed at zero and 5000 r.p.m. and considering various torque from 0 to 100,000 N m. The natural frequencies calculated for the first four modes of 0 and 5000 r.p.m. are listed in Tables 4 and 5 respectively. As the torque increases, the natural frequency decreases in the calculated four modes. In the presence of torque, the eigenvalues are complex values and the mode shapes are in a twisted plane out of a flat plane. The mode shapes calculated for shaft rotation speed 5000 r.p.m. and applied torque 100,000 N m are shown in Figure 3. In this figure, (a) is the amplitude of the modes and (b) is the twisting angle with a 360° tic mark interval.

TABLE 4
Natural frequencies of the multi-step shaft with applied torque ($\Omega = 0$)

Torque (N m)	Natural frequencies (r.p.m.)			
	1st mode	2nd mode	3rd mode	4th mode
0–100	16120·7	66246·1	144707·4	252016·8
1000	16120·7	66246·0	144707·3	252016·7
10000	16118·4	66242·8	144703·7	252013·0
100000	15888·6	65918·0	144342·3	251633·8

TABLE 5
Natural frequencies of the multi-step shaft with applied torque ($\Omega = 5000$ *r.p.m.*)

Torque (N m)	Natural frequencies (r.p.m.)							
	1st mode		2nd mode		3rd mode		4th mode	
	Backward	Forward	Backward	Forward	Backward	Forward	Backward	Forward
0–100	16099·9	16141·4	66144·5	66347·8	144549·6	144865·2	251706·0	252327·8
1000	16099·9	16141·4	66144·5	66347·7	144549·6	144865·2	251705·9	252327·7
10000	16097·6	16139·2	66141·2	66344·5	144546·0	144861·6	251702·2	252324·0
100000	15867·6	15909·6	65816·3	66019·9	144184·5	144500·2	251322·6	251945·2

4.4. MODE SHEAR FORCE AND BENDING MOMENT CURVES

The mode shapes shown in Figure 2 have numerically differentiated with respect to the axial co-ordinate. The derivatives have been substituted into equation (17) to yield shear force and bending moment distribution curves shown in Figures 4 and 5 respectively.

The nodes and anti-nodes of shear force distribution of Figure 4 correspond to the anti-nodes and nodes respectively of the natural mode shapes. Meanwhile, the bending moment distribution of Figure 5 shows a trend similar to the natural mode shapes. The calculation of mode shear force and bending moment curves as well as the natural mode shapes can be used for evaluating the stress distribution, and hence for trouble-shooting and design.

5. CONCLUSION

Bending vibrations of a rotating shaft with a discontinuously varying cross-section have been analytically studied by using the Timoshenko beam theory including rotary inertia and shear deformation. Torque has been considered as in

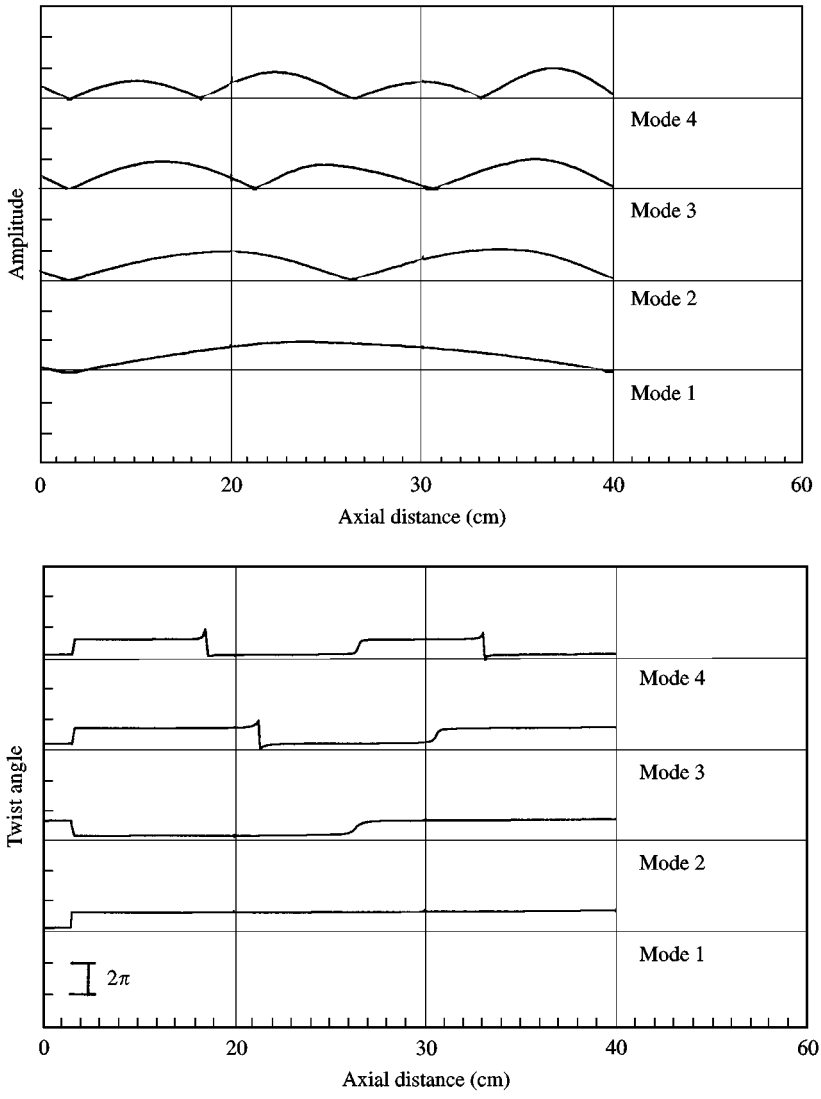

Figure 3. Mode shapes of the first four natural modes of bending vibration (rotation speed 5000 r.p.m., applied torque 100,000 N m): (a) normalized mode amplitude, (b) twist angle of mode plane.

a power-transmission shaft and the gyroscopic effect due to the shaft rotation also has been included in the equation of motion.

In contrast to numerical analysis such as the finite element method, the analysis presented in this paper uses the differential equation of motion for a continuous system and obtains solutions by applying boundary conditions. The fourth order partial differential equation has been transformed into an ordinary differential equation by expressing two vertical displacement components as one complex variable and introducing separation of time and spatial variables. A system of algebraic equations resulting from the ordinary differential equations with assumed

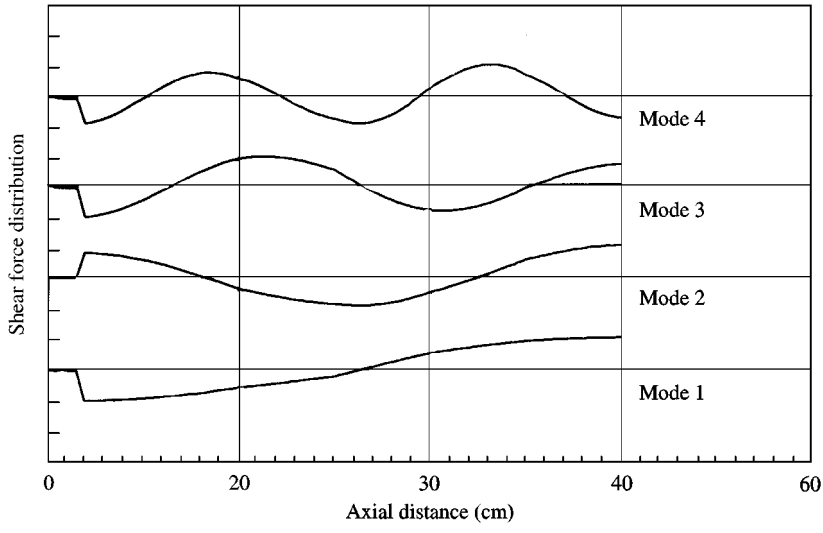

Figure 4. Shear force distribution of the first four modes.

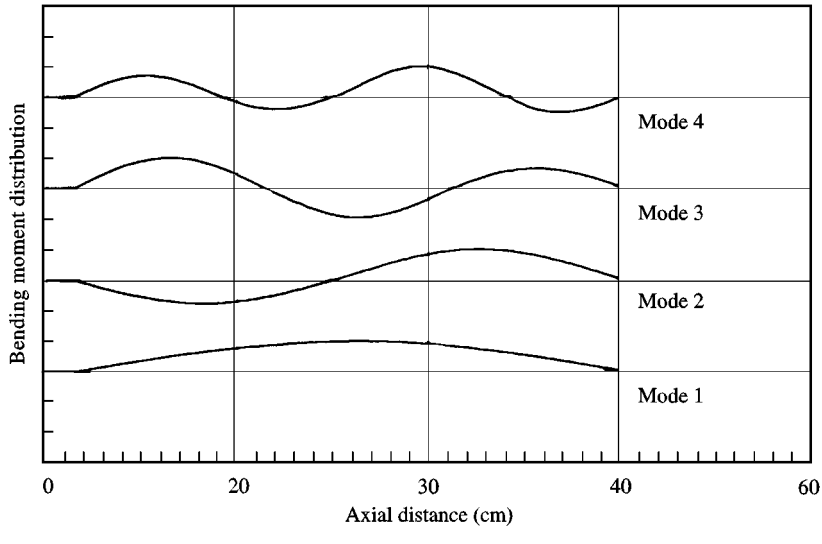

Figure 5. Bending moment distribution of the first four modes.

forms of solutions and boundary conditions have yielded natural frequencies and modes.

The accuracy of the analysis method has been confirmed by calculating the natural frequencies of a stationary uniform shaft with no torque and comparing them with the corresponding values obtained from the Euler–Bernoulli beam theory. The natural frequencies of a rotating multi-step shaft have been calculated for forward and backward precession. The comparison with the results obtained

using the finite element method shows a bigger error for a higher mode in the FEM result. The analysis has been applied to the rotating multi-step shaft with torque, and has yielded natural frequencies and modes as a form of continuous curve.

The effect of the torque applied at each end of the shaft changes the characteristics of natural vibration of the rotating shaft. The change of the natural frequencies due to the applied torque is in the decreasing direction in all modes at a given rotating speed. In the presence of the torque, the mode shapes appear in a twisted plane out of a flat plane.

The analysis method presented in this paper has yielded accurately the natural vibration characteristics of a rotating multi-step shaft with torque. In contrast to the finite element method, this method has obtained a continuous mode-shape curve, and hence it can provide shear force and bending moment distribution.

ACKNOWLEDGMENT

The authors thank Prof. S.-W. Hong for the FEM calculation and Prof. C.-W. Lee for the helpful discussions. This work was partially supported by a grant from the Critical Technology 21 Project of the Ministry of Science and Technology, Korea.

REFERENCES

1. P. Y. Kim, R. C. Flanagan and I. R. G. Lowe 1989 *Rotating Machinery Dynamics, ASME Publication DE* **18**, 71–76. A new method for the critical speed calculation of rotor-bearing systems—part I: theory.
2. O. S. Jun and P. Y. Kim 1994 *Proceedings of the International Conference on Vibration Engineering, Beijing*, 759–764. A method for torsional critical speed calculation of practical industrial rotors.
3. D. J. Inman 1996 *Engineering Vibration*, Englewood Cliffs, NJ: Prentice-Hall, Inc. Chapter 6.
4. C.-W. Lee 1993 *Vibration Analysis of Rotors*, The Netherlands: Kluwer Academic Publishers. Chapter 8.
5. W. H. Beyer 1979 *CRC Standard Mathematical Tables*. U.S.A: CRC Press Inc.

APPENDIX A

The boundary conditions at specified boundaries and interfaces are as follows. These have been derived from equations 17(a–d).

Free left end (1st node):

$$\begin{bmatrix} EI_1\lambda_{11}^2 - \mathrm{j}T\lambda_{11} \\ EI_1\lambda_{12}^2 - \mathrm{j}T\lambda_{12} \\ EI_1\lambda_{13}^2 - \mathrm{j}T\lambda_{13} \\ EI_1\lambda_{14}^2 - \mathrm{j}T\lambda_{14} \end{bmatrix}^T \begin{bmatrix} p_{11} \\ p_{12} \\ p_{13} \\ p_{14} \end{bmatrix} = 0, \tag{A1a}$$

$$\begin{bmatrix} EI_1\lambda_{11}^3 + \rho A_1 r_{1o}^2(\omega^2 - 2\omega\Omega)\lambda_{11} - \mathrm{j}T\lambda_{11}^2 \\ EI_1\lambda_{12}^3 + \rho A_1 r_{1o}^2(\omega^2 - 2\omega\Omega)\lambda_{12} - \mathrm{j}T\lambda_{12}^2 \\ EI_1\lambda_{13}^3 + \rho A_1 r_{1o}^2(\omega^2 - 2\omega\Omega)\lambda_{13} - \mathrm{j}T\lambda_{13}^2 \\ EI_1\lambda_{14}^3 + \rho A_1 r_{1o}^2(\omega^2 - 2\omega\Omega)\lambda_{14} - \mathrm{j}T\lambda_{14}^2 \end{bmatrix}^T \begin{bmatrix} p_{11} \\ p_{12} \\ p_{13} \\ p_{14} \end{bmatrix} = 0. \tag{A1b}$$

Free right end ($(N+1)$th node located in the Nth shaft step):

$$\begin{bmatrix} (EI_N\lambda_{N1}^2 - \mathrm{j}T\lambda_{N1})\mathrm{e}^{\lambda_{N1}l_{N+1}} \\ (EI_N\lambda_{N2}^2 - \mathrm{j}T\lambda_{N2})\mathrm{e}^{\lambda_{N2}l_{N+1}} \\ (EI_N\lambda_{N3}^2 - \mathrm{j}T\lambda_{N3})\mathrm{e}^{\lambda_{N3}l_{N+1}} \\ (EI_N\lambda_{N4}^2 - \mathrm{j}T\lambda_{N4})\mathrm{e}^{\lambda_{N4}l_{N+1}} \end{bmatrix}^T \begin{bmatrix} p_{N1} \\ p_{N2} \\ p_{N3} \\ p_{N4} \end{bmatrix} = 0, \tag{A2a}$$

$$\begin{bmatrix} (EI_N\lambda_{N1}^3 + \rho A_N r_{No}^2(\omega^2 - 2\omega\Omega)\lambda_{N1} - \mathrm{j}T\lambda_{N1}^2)\mathrm{e}^{\lambda_{N1}l_{N+1}} \\ (EI_N\lambda_{N2}^3 + \rho A_N r_{No}^2(\omega^2 - 2\omega\Omega)\lambda_{N2} - \mathrm{j}T\lambda_{N2}^2)\mathrm{e}^{\lambda_{N2}l_{N+1}} \\ (EI_N\lambda_{N3}^3 + \rho A_N r_{No}^2(\omega^2 - 2\omega\Omega)\lambda_{N3} - \mathrm{j}T\lambda_{N3}^2)\mathrm{e}^{\lambda_{N3}l_{N+1}} \\ (EI_N\lambda_{N4}^3 + \rho A_N r_{No}^2(\omega^2 - 2\omega\Omega)\lambda_{N4} - \mathrm{j}T\lambda_{N4}^2)\mathrm{e}^{\lambda_{N4}l_{N+1}} \end{bmatrix}^T \begin{bmatrix} p_{N1} \\ p_{N2} \\ p_{N3} \\ p_{N4} \end{bmatrix} = 0. \tag{A2b}$$

Cross-section jump (nth node):

$$\begin{bmatrix} \mathrm{e}^{\lambda_{(n-1)1}l_n} \\ \mathrm{e}^{\lambda_{(n-1)2}l_n} \\ \mathrm{e}^{\lambda_{(n-1)3}l_n} \\ \mathrm{e}^{\lambda_{(n-1)4}l_n} \\ -\mathrm{e}^{\lambda_{n1}l_n} \\ -\mathrm{e}^{\lambda_{n2}l_n} \\ -\mathrm{e}^{\lambda_{n3}l_n} \\ -\mathrm{e}^{\lambda_{n4}l_n} \end{bmatrix}^T \begin{bmatrix} p_{(n-1)1} \\ p_{(n-1)2} \\ p_{(n-1)3} \\ p_{(n-1)4} \\ p_{n1} \\ p_{n2} \\ p_{n3} \\ p_{n4} \end{bmatrix} = 0, \tag{A3a}$$

$$\begin{bmatrix} \lambda_{(n-1)1}\mathrm{e}^{\lambda_{(n-1)1}l_n} \\ \lambda_{(n-1)2}\mathrm{e}^{\lambda_{(n-1)2}l_n} \\ \lambda_{(n-1)3}\mathrm{e}^{\lambda_{(n-1)3}l_n} \\ \lambda_{(n-1)4}\mathrm{e}^{\lambda_{(n-1)4}l_n} \\ -\lambda_{n1}\mathrm{e}^{\lambda_{n1}l_n} \\ -\lambda_{n2}\mathrm{e}^{\lambda_{n2}l_n} \\ -\lambda_{n3}\mathrm{e}^{\lambda_{n3}l_n} \\ -\lambda_{n4}\mathrm{e}^{\lambda_{n4}l_n} \end{bmatrix}^T \begin{bmatrix} p_{(n-1)1} \\ p_{(n-1)2} \\ p_{(n-1)3} \\ p_{(n-1)4} \\ p_{n1} \\ p_{n2} \\ p_{n3} \\ p_{n4} \end{bmatrix} = 0, \tag{A3b}$$

$$\begin{bmatrix} (EI_{n-1}\lambda_{(n-1)1}^2 - \mathrm{j}T\lambda_{(n-1)1})\mathrm{e}^{\lambda_{(n-1)1}l_n} \\ (EI_{n-1}\lambda_{(n-1)2}^2 - \mathrm{j}T\lambda_{(n-1)2})\mathrm{e}^{\lambda_{(n-1)2}l_n} \\ (EI_{n-1}\lambda_{(n-1)3}^2 - \mathrm{j}T\lambda_{(n-1)3})\mathrm{e}^{\lambda_{(n-1)3}l_n} \\ (EI_{n-1}\lambda_{(n-1)4}^2 - \mathrm{j}T\lambda_{(n-1)4})\mathrm{e}^{\lambda_{(n-1)4}l_n} \\ -(EI_n\lambda_{n1}^2 - \mathrm{j}T\lambda_{n1})\mathrm{e}^{\lambda_{n1}l_n} \\ -(EI_n\lambda_{n2}^2 - \mathrm{j}T\lambda_{n2})\mathrm{e}^{\lambda_{n2}l_n} \\ -(EI_n\lambda_{n3}^2 - \mathrm{j}T\lambda_{n3})\mathrm{e}^{\lambda_{n3}l_n} \\ -(EI_n\lambda_{n4}^2 - \mathrm{j}T\lambda_{n4})\mathrm{e}^{\lambda_{n4}l_n} \end{bmatrix}^T \begin{bmatrix} p_{(n-1)1} \\ p_{(n-1)2} \\ p_{(n-1)3} \\ p_{(n-1)4} \\ p_{n1} \\ p_{n2} \\ p_{n3} \\ p_{n4} \end{bmatrix} = 0, \tag{A3c}$$

$$\begin{bmatrix} (EI_{n-1}\lambda_{(n-1)1}^3 + \rho A_{n-1}r_{(n-1)o}^2(\omega^2 - 2\omega\Omega)\lambda_{(n-1)1} - \mathrm{j}T\lambda_{(n-1)1}^2)\mathrm{e}^{\lambda_{(n-1)1}l_n} \\ (EI_{n-1}\lambda_{(n-1)2}^3 + \rho A_{n-1}r_{(n-1)o}^2(\omega^2 - 2\omega\Omega)\lambda_{(n-1)2} - \mathrm{j}T\lambda_{(n-1)2}^2)\mathrm{e}^{\lambda_{(n-1)2}l_n} \\ (EI_{n-1}\lambda_{(n-1)3}^3 + \rho A_{n-1}r_{(n-1)o}^2(\omega^2 - 2\omega\Omega)\lambda_{(n-1)3} - \mathrm{j}T\lambda_{(n-1)3}^2)\mathrm{e}^{\lambda_{(n-1)3}l_n} \\ (EI_{n-1}\lambda_{(n-1)4}^3 + \rho A_{n-1}r_{(n-1)o}^2(\omega^2 - 2\omega\Omega)\lambda_{(n-1)4} - \mathrm{j}T\lambda_{(n-1)4}^2)\mathrm{e}^{\lambda_{(n-1)4}l_n} \\ -(EI_n\lambda_{n1}^3 + \rho A_n r_{no}^2(\omega^2 - 2\omega\Omega)\lambda_{n1} - \mathrm{j}T\lambda_{n1}^2)\mathrm{e}^{\lambda_{n1}l_n} \\ -(EI_n\lambda_{n2}^3 + \rho A_n r_{no}^2(\omega^2 - 2\omega\Omega)\lambda_{n2} - \mathrm{j}T\lambda_{n2}^2)\mathrm{e}^{\lambda_{n2}l_n} \\ -(EI_n\lambda_{n3}^3 + \rho A_n r_{no}^2(\omega^2 - 2\omega\Omega)\lambda_{n3} - \mathrm{j}T\lambda_{n3}^2)\mathrm{e}^{\lambda_{n3}l_n} \\ -(EI_n\lambda_{n4}^3 + \rho A_n r_{no}^2(\omega^2 - 2\omega\Omega)\lambda_{n4} - \mathrm{j}T\lambda_{n4}^2)\mathrm{e}^{\lambda_{n4}l_n} \end{bmatrix}^T$$

$$\times \begin{bmatrix} p_{(n-1)1} \\ p_{(n-1)2} \\ p_{(n-1)3} \\ p_{(n-1)4} \\ p_{n1} \\ p_{n2} \\ p_{n3} \\ p_{n4} \end{bmatrix} = 0, \tag{A3d}$$

Radially rigid bearing (nth node):

$$\begin{bmatrix} \mathrm{e}^{\lambda_{(n-1)1}l_n} \\ \mathrm{e}^{\lambda_{(n-1)2}l_n} \\ \mathrm{e}^{\lambda_{(n-1)3}l_n} \\ \mathrm{e}^{\lambda_{(n-1)4}l_n} \\ -\mathrm{e}^{\lambda_{n1}l_n} \\ -\mathrm{e}^{\lambda_{n2}l_n} \\ -\mathrm{e}^{\lambda_{n3}l_n} \\ -\mathrm{e}^{\lambda_{n4}l_n} \end{bmatrix}^T \begin{bmatrix} p_{(n-1)1} \\ p_{(n-1)2} \\ p_{(n-1)3} \\ p_{(n-1)4} \\ p_{n1} \\ p_{n2} \\ p_{n3} \\ p_{n4} \end{bmatrix} = 0, \tag{A4a}$$

$$\begin{bmatrix} \lambda_{(n-1)1}\mathrm{e}^{\lambda_{(n-1)1}l_n} \\ \lambda_{(n-1)2}\mathrm{e}^{\lambda_{(n-1)2}l_n} \\ \lambda_{(n-1)3}\mathrm{e}^{\lambda_{(n-1)3}l_n} \\ \lambda_{(n-1)4}\mathrm{e}^{\lambda_{(n-1)4}l_n} \\ -\lambda_{n1}\mathrm{e}^{\lambda_{n1}l_n} \\ -\lambda_{n2}\mathrm{e}^{\lambda_{n2}l_n} \\ -\lambda_{n3}\mathrm{e}^{\lambda_{n3}l_n} \\ -\lambda_{n4}\mathrm{e}^{\lambda_{n4}l_n} \end{bmatrix}^T \begin{bmatrix} p_{(n-1)1} \\ p_{(n-1)2} \\ p_{(n-1)3} \\ p_{(n-1)4} \\ p_{n1} \\ p_{n2} \\ p_{n3} \\ p_{n4} \end{bmatrix} = 0, \tag{A4b}$$

$$\begin{bmatrix} (EI_{n-1}\lambda_{(n-1)1}^2 - \mathrm{j}T\lambda_{(n-1)1})\mathrm{e}^{\lambda_{(n-1)1}l_n} \\ (EI_{n-1}\lambda_{(n-1)2}^2 - \mathrm{j}T\lambda_{(n-1)2})\mathrm{e}^{\lambda_{(n-1)2}l_n} \\ (EI_{n-1}\lambda_{(n-1)3}^2 - \mathrm{j}T\lambda_{(n-1)3})\mathrm{e}^{\lambda_{(n-1)3}l_n} \\ (EI_{n-1}\lambda_{(n-1)4}^2 - \mathrm{j}T\lambda_{(n-1)4})\mathrm{e}^{\lambda_{(n-1)4}l_n} \\ -(EI_n\lambda_{n1}^2 - \mathrm{j}T\lambda_{n1})\mathrm{e}^{\lambda_{n1}l_n} \\ -(EI_n\lambda_{n2}^2 - \mathrm{j}T\lambda_{n2})\mathrm{e}^{\lambda_{n2}l_n} \\ -(EI_n\lambda_{n3}^2 - \mathrm{j}T\lambda_{n3})\mathrm{e}^{\lambda_{n3}l_n} \\ -(EI_n\lambda_{n4}^2 - \mathrm{j}T\lambda_{n4})\mathrm{e}^{\lambda_{n4}l_n} \end{bmatrix}^T \begin{bmatrix} p_{(n-1)1} \\ p_{(n-1)2} \\ p_{(n-1)3} \\ p_{(n-1)4} \\ p_{n1} \\ p_{n2} \\ p_{n3} \\ p_{n4} \end{bmatrix} = 0, \tag{A4c}$$

$$\begin{bmatrix} (EI_{n-1}\lambda_{(n-1)1}^3 + \rho A_{n-1}r_{(n-1)o}^2(\omega^2 - 2\omega\Omega)\lambda_{(n-1)1} - \mathrm{j}T\lambda_{(n-1)1}^2 - K)\mathrm{e}^{\lambda_{(n-1)1}l_n} \\ (EI_{n-1}\lambda_{(n-1)2}^3 + \rho A_{n-1}r_{(n-1)o}^2(\omega^2 - 2\omega\Omega)\lambda_{(n-1)2} - \mathrm{j}T\lambda_{(n-1)2}^2 - K)\mathrm{e}^{\lambda_{(n-1)2}l_n} \\ (EI_{n-1}\lambda_{(n-1)3}^3 + \rho A_{n-1}r_{(n-1)o}^2(\omega^2 - 2\omega\Omega)\lambda_{(n-1)3} - \mathrm{j}T\lambda_{(n-1)3}^2 - K)\mathrm{e}^{\lambda_{(n-1)3}l_n} \\ (EI_{n-1}\lambda_{(n-1)4}^3 + \rho A_{n-1}r_{(n-1)o}^2(\omega^2 - 2\omega\Omega)\lambda_{(n-1)4} - \mathrm{j}T\lambda_{(n-1)4}^2 - K)\mathrm{e}^{\lambda_{(n-1)4}l_n} \\ -(EI_n\lambda_{n1}^3 + \rho A_n r_{no}^2(\omega^2 - 2\omega\Omega)\lambda_{n1} - \mathrm{j}T\lambda_{n1}^2)\mathrm{e}^{\lambda_{n1}l_n} \\ -(EI_n\lambda_{n2}^3 + \rho A_n r_{no}^2(\omega^2 - 2\omega\Omega)\lambda_{n2} - \mathrm{j}T\lambda_{n2}^2)\mathrm{e}^{\lambda_{n2}l_n} \\ -(EI_n\lambda_{n3}^3 + \rho A_n r_{no}^2(\omega^2 - 2\omega\Omega)\lambda_{n3} - \mathrm{j}T\lambda_{n3}^2)\mathrm{e}^{\lambda_{n3}l_n} \\ -(EI_n\lambda_{n4}^3 + \rho A_n r_{no}^2(\omega^2 - 2\omega\Omega)\lambda_{n4} - \mathrm{j}T\lambda_{n4}^2)\mathrm{e}^{\lambda_{n4}l_n} \end{bmatrix}^T$$

$$\times \begin{bmatrix} p_{(n-1)1} \\ p_{(n-1)2} \\ p_{(n-1)3} \\ p_{(n-1)4} \\ p_{n1} \\ p_{n2} \\ p_{n3} \\ p_{n4} \end{bmatrix} = 0, \tag{A4d}$$

Radially rigid bearing at the left end (1st node):

$$\begin{bmatrix} EI_1\lambda_{11}^2 - \mathrm{j}T\lambda_{11} \\ EI_1\lambda_{12}^2 - \mathrm{j}T\lambda_{12} \\ EI_1\lambda_{13}^2 - \mathrm{j}T\lambda_{13} \\ EI_1\lambda_{14}^2 - \mathrm{j}T\lambda_{14} \end{bmatrix}^T \begin{bmatrix} p_{11} \\ p_{12} \\ p_{13} \\ p_{14} \end{bmatrix} = 0, \tag{A5a}$$

$$\begin{bmatrix} -K - (EI_1\lambda_{11}^3 + \rho A_1 r_{1o}^2(\omega^2 - 2\omega\Omega)\lambda_{11} - \mathrm{j}T\lambda_{11}^2) \\ -K - (EI_1\lambda_{12}^3 + \rho A_1 r_{1o}^2(\omega^2 - 2\omega\Omega)\lambda_{12} - \mathrm{j}T\lambda_{12}^2) \\ -K - (EI_1\lambda_{13}^3 + \rho A_1 r_{1o}^2(\omega^2 - 2\omega\Omega)\lambda_{13} - \mathrm{j}T\lambda_{13}^2) \\ -K - (EI_1\lambda_{14}^3 + \rho A_1 r_{1o}^2(\omega^2 - 2\omega\Omega)\lambda_{14} - \mathrm{j}T\lambda_{14}^2) \end{bmatrix}^T \begin{bmatrix} p_{11} \\ p_{12} \\ p_{13} \\ p_{14} \end{bmatrix} = 0. \tag{A5b}$$

Radially rigid bearing at the right end ($(N+1)$th node):

$$\begin{bmatrix} (EI_N\lambda_{N1}^2 - \mathrm{j}T\lambda_{N1})\mathrm{e}^{\lambda_{N1}l_{N+1}} \\ (EI_N\lambda_{N2}^2 - \mathrm{j}T\lambda_{N2})\mathrm{e}^{\lambda_{N2}l_{N+1}} \\ (EI_N\lambda_{N3}^2 - \mathrm{j}T\lambda_{N3})\mathrm{e}^{\lambda_{N3}l_{N+1}} \\ (EI_N\lambda_{N4}^2 - \mathrm{j}T\lambda_{N4})\mathrm{e}^{\lambda_{N4}l_{N+1}} \end{bmatrix}^T \begin{bmatrix} p_{N1} \\ p_{N2} \\ p_{N3} \\ p_{N4} \end{bmatrix} = 0, \tag{A6a}$$

$$\begin{bmatrix} (EI_N\lambda_{N1}^3 + \rho A_N r_{No}^2(\omega^2 - 2\omega\Omega)\lambda_{N1} - \mathrm{j}T\lambda_{N1}^2 - K)\mathrm{e}^{\lambda_{N1}l_{N+1}} \\ (EI_N\lambda_{N2}^3 + \rho A_N r_{No}^2(\omega^2 - 2\omega\Omega)\lambda_{N2} - \mathrm{j}T\lambda_{N2}^2 - K)\mathrm{e}^{\lambda_{N2}l_{N+1}} \\ (EI_N\lambda_{N3}^3 + \rho A_N r_{No}^2(\omega^2 - 2\omega\Omega)\lambda_{N3} - \mathrm{j}T\lambda_{N3}^2 - K)\mathrm{e}^{\lambda_{N3}l_{N+1}} \\ (EI_N\lambda_{N4}^3 + \rho A_N r_{No}^2(\omega^2 - 2\omega\Omega)\lambda_{N4} - \mathrm{j}T\lambda_{N4}^2 - K)\mathrm{e}^{\lambda_{N4}l_{N+1}} \end{bmatrix}^T \begin{bmatrix} p_{N1} \\ p_{N2} \\ p_{N3} \\ p_{N4} \end{bmatrix} = 0. \tag{A6b}$$